Highly efficient mixed Li^+ transport in ion gel polycationic electrolytes

Jesús L. Pablos, N. García, L. Garrido, J. Guzmán, F. Catalina, T. Corrales, P. Tiemblo

Instituto de Ciencia y Tecnología de Polímeros, Consejo Superior de Investigaciones Científicas, ICTP-CSIC, Juan de la Cierva 3, 28006 Madrid, Spain

Abstract

Outstanding Li^+ conductivity and diffusivity have been achieved in free-standing ion gel electrolytes synthesized by in-situ photopolymerization of 1-(2-methacryloyloxy)ethyl-3-butylimidazolium bis(trifluoromethane sulfonyl)imide (IMMA) and/or poly(ethylene glycol) methacrylate (EGMA), in the presence of the room temperature ionic liquids 1-ethyl-3-methylimidazolium bis(fluorosulfonyl)imide (EMIFSI), 1-butyl-1-methylpyrrolidinium bis(fluorosulfonyl)imide (BMPFSI) and bis(trifluoromethane)sulfonimide lithium salt (LiTFSI). The membranes are easy to handle and thermally stable up to 200 ºC. Those containing IMMA in the polymer chain present liquid-like ionic conductivities (up to 10 mS cm^{-1} at 25 ºC), and liquid-like Li^+ diffusivities and conductivities ($D_{Li} \approx 4 \times 10^{-11}$ m^2 s^{-1}, $\sigma_{Li} \approx 1.4$ mS cm^{-1} at 25 ºC) unreported so far in a solid electrolyte. D_{Li} is not only very high but significantly higher than its counteranions' diffusivity, D_{FSI} or D_{TFSI}, a very rare behavior in electrolytes where transport is, in principle, ruled by viscosity. It is proposed that in these polycationic electrolytes the motion of Li^+ occurs via two different transport mechanisms, the well-known viscosity-governed transport and an additional anion-exchange mechanism that enables very fast Li^+ diffusion. This combination has high practical relevance for Li^+ batteries as it implies a high contribution of σ_{Li} to the overall electrolyte's conductivity, and it constitutes a breakthrough in the design of polymer-based solid electrolytes for Li.

Keywords: Li-ion transport, polycationic electrolytes, ion gel electrolytes, polymerizable ionic liquids, anion-exchange transport

1. Introduction

The design of solid electrolytes with electrochemical characteristics comparable to those of liquid ones is a very challenging endeavor for materials scientists, for it requires producing a self-standing material with a local mobility comparable to that of a liquid. Such a material must combine high ionic diffusivity (and hence high ionic conductivity) and dimensional stability, and for the last decade the best candidates have been polymer based materials.[1] Solid polymer electrolytes include polymer 3D networks swollen with ad-hoc liquids[2, 3] to produce chemically [1] or physically crosslinked gels.[4-6] For the sake of electrochemical and thermal stability in the last years the soaking liquid has frequently been a room temperature ionic liquid (RTIL).[7, 8] Particularly interesting for electrochemical applications are RTILs containing bis(fluorosulfonyl)imide anion (FSI), because of its low viscosity, and because it has been demonstrated that the viscosity increase arising from the incorporation of a Li salt to an ionic liquid is much lower when the anion is FSI.[9]

To date, the highest reported conductivity in a polymer gel electrolyte with RTIL (N-methyl-N-propylpyrrolidinium bis(fluorosulfonyl)imide, PMPFSI) has been 1.6 mS cm^{-1} at 20 ºC [10], of which only a small part is actually Li ion conductivity. As Li^+ has a characteristic large solvation shell [11] D_{Li} is smaller than its counteranions,[12, 13] most frequently FSI or bis(trifluoromethane)sulfonimide (TFSI), and hence the contribution of Li to the overall conductivity is small. In this connection, polymer ion gels where the polymer scaffold is a polyelectrolyte made of a polymerizable ionic liquid are of great interest,[12, 14] not only because of their well-known advantages as regards safety, but because polycationic scaffolds seem to enhance Li^+ mobility (diffusivity) under certain conditions.[13] On the other hand, in liquid Li^+ electrolytes containing the FSI anion some authors[15, 16] have recently found that for Li^+ electrolytes containing FSI D_{Li} can be slightly higher than D_{FSI} (≈ a 10%) at sufficiently high temperature and high Li salt concentration. In these works, it is proposed that an anion exchange

transport mechanism appears that increases the Li^+ mobility with respect to the rest of ions in the electrolyte.[17]

In the light of the Li^+ mobility enhancement promoted by both polycationic scaffolds and the presence of the anion FSI in the liquid phase of the electrolyte, in this work we present free standing ion gel electrolytes which consist of crosslinked polymethacrylates with imidazolium pendant groups and RTILs containing FSI as liquid phase. These new self-standing ion gels present a combination of properties unreported to date, with ionic conductivity and D_{Li} significantly higher than analogous liquid electrolytes[16] and where D_{Li} is up to a 40% higher than D_{FSI} (and 80% higher than D_{TFSI}) at 25 ºC.

2. Experimental part

2.1 Materials and methods

2.1.1. Materials

All reactants and solvents were commercially available and used as received: 2-bromoethanol (Aldrich, 95 %), triethylamine (Sigma Aldrich, 99%), methacryloyl chloride (Aldrich, 97 %), 1-butylimidazole (Aldrich, 98 %), hydroquinone (Panreac, 99.5 %), poly(ethylene glycol) methylether methacrylate (Aldrich, Average Mn 300), ethyleneglycol dimethacrylate (Aldrich, 98 %), 1-ethyl-3-methylimidazolium bis(fluorosulfonyl)imide (Solvionic, 99.5 %), 1-butyl-1-methylpyrrolidinium bis(fluorosulfonyl)imide (Solvionic, 99.5 %), bis(trifluoromethane)sulfonamide lithium salt (Aldrich, 99.95 %), milliQ water, dichloromethane (Aldrich, 99.99 %), hexane (Scharlau, 99.8 %). %). $[^{13}C]O_2$ labeled 99% was of Cambridge Isotopes Laboratories, Andover, MA.

2.1.2. Synthesis of 1-(2-methacryloyloxy)ethyl-3-butylimidazolium bis(trifluoromethane sulfonyl)imide) (**IMMA**).

2.1.2.1.Synthesis of 2-bromoethyl methacrylate (**M1***)*[18, 19] In an ace round-bottom pressure flask a solution of 2- bromoethanol (7.0 g, 0.055 mol) in 75 mL of

dichloromethane was added. Then, a solution of methacryloyl chloride (5.6 mL, 0.06 mol) in 5 mL of dichloromethane was gradually added to the mixture at 0 °C over 10 min. After addition, the reaction mixture was continuously stirred for 30 min and triethylamine (4.04 mL, 0.06 mol) in 4 mL of dichloromethane was added dropwise at 0°C for 15 min. The reaction mixture was stirred overnight at room temperature and then filtered. The filtrate was washed thoroughly using 3×100 mL of deionized H_2O and dried by anhydrous magnesium sulfate. The solvent was removed under vacuum below 30°C. Yield: 8.92 g (85%) (**M1**). ^{1}H-NMR (400 MHz, CDCl3): δ (ppm) 6.12 (s, 1H), 5.57 (s, 1H), 4.40 (t, *J* = 6.1 Hz, 2H), 3.51 (t, *J* = 6.1 Hz, 2H), 1.91 (s, 3H). ^{13}C NMR (400 MHz, $CDCl_3$) δ (ppm) 166.74, 135.82, 126.23, 63.96, 28.80, 18.20. FTIR (wavenumber, cm^{-1}): st(C=O) 1718; st(C=C) 1637; st (C-O) 1153.

2.1.2.2.Synthesis of 1-(2-methacryloyloxy)ethyl-3-butylimidazolium bromide (**M2**).[20] In an ace round-bottom pressure flask, a mixture of 2-bromoethyl methacrylate (**M1**) (1 g., 0.008 mol) and *1*-butylimidazole (1.55 g., 0.008 mol) with a small amount of hydroquinone to inhibit the thermal polymerization of the resulting monomer, was stirred at 40 ºC for 72 hours. The reaction mixture was dissolved in 5 mL of dichloromethane and poured into 250 ml of hexane to give a viscous white precipitate. The product was collected and dried in vacuum. Yield: 2.28 g. (90 %) (**M2**). ^{1}H-NMR (400 MHz, DMSO-d_6): δ (ppm) 9.52 (s, 1H), 7.92 (m, 2H), 6.02 (s, 1H), 5.68 (s, 1H), 4.64 – 4.57 (m, 2H), 4.52 – 4.41 (m, 2H), 4.23 (t, *J* = 7.0 Hz, 2H), 1.76 (s, 3H), 1.21 (m, 2H), 0.85 (t, *J* = 7.3 Hz, 3H). ^{13}C NMR (400 MHz, DMSO-d_6) δ (ppm) 165.91, 136.55, 135.10, 126.56, 122.73, 122.52, 62.49, 48.56, 47.98, 31.31, 18.62, 17.80, 13.18. FTIR (wavenumbers, cm^{-1}): st(C=O) 1718; st(C=C) 1637; st (C-O) 1155; st (C=C) 1559; st (C=N) 1452; st (C-N) 1297; st (C-H) 2940; st(=-C-H) 3200-3000.

2.1.2.3.Synthesis of 1-(2-methacryloyloxy)ethyl-3-butylimidazolium bis(trifluoromethane sulfonyl)imide **(IMMA)**[20] In an ace round-bottom pressure flask, a mixture of **M2** (1.69 g., 0.0053 mol) and bis(trifluoromethane) sulfonimide lithium salt (LiTFSI, 1.40 g., 0.0048 mol) were diluted in 80 ml of milliQ H_2O, and was stirred at 25ºC for 3 days to

induce a liquid-liquid phase separation. The organic layer was isolated and diluted with dichloromethane (15 mL). This solution was washed with water (3 × 30 mL). The product was concentrated under reduced pressure to obtain a viscous light brown oil, **IMMA**. Yield: 2.1 g. (77 %). ^{1}H-NMR (400 MHz, DMSO-d_6): δ (ppm) 9.24 (s, 1H), 7.80 (m, 2H), 6.03 (s, 1H), 5.69 (s, 1H), 4.52 (m, 2H), 4.48 (m, 2H), 4.19 (t, *J* = 7.0 Hz, 2H), 1.84 (s, 3H), 1.76 (m, 2H), 1.24 (m, 2H), 0.89 (t, *J* = 7.3 Hz, 3H). ^{13}C NMR (400 MHz, DMSO-d_6) δ (ppm) δ 165.96, 136.52, 135.24, 126.40, 122.84, 122.54, 62.40, 48.73, 48.12, 31.33, 18.68, 17.73, 13.06. Quartet arising from CF_3 in the TFSI anion 124.31, 121.11, 117.91, 114.7. FTIR (wavenumbers, cm^{-1}): st(C=O) 1726; st(C=C) 1640; st (C-O) 1153; st (C=C) 1559; st (C=N) 1460; st (C-N) 1295; st (C-H) 2970; st(=-C-H) 3150-3000.

2.1.3. Synthesis of the gel electrolytes

The conductive gel electrolytes were prepared by radical polymerization of IMMA and/or poly(ethylene glycol) methylether methacrylate (EGMA) using ethylene glycol dimethacrylate (EGDMMA) as cross-linking agent (1 wt.%), Irgacure 651 (1 wt.%) as photo-initiator and in the presence of LiTFSI and EMIFSI or mixtures of EMIFSI/BMPFSI(see the different compositions in Table 1). The homogenous solution comprising all components, were transferred to a glass vial, degassed by nitrogen bubbling and ultrasounds for 10 min. After that, 825 µL of the mixture was injected into an oxygen-free atmosphere in a circular teflon mould of 2.5 cm of diameter. In this mould, the photoinitiated bulk polymerization was performed by irradiation with UV light (365 nm) at RT for 55 minutes. Then, the gel electrolyte was demoulded and conditioned at RT. GPEs of ≈ 1300 µm thick were obtained. The chemical structures of all the components are depicted in Scheme I. More details on the composition, thermal stability and rheology of the gel electrolytes appear in Table 1.

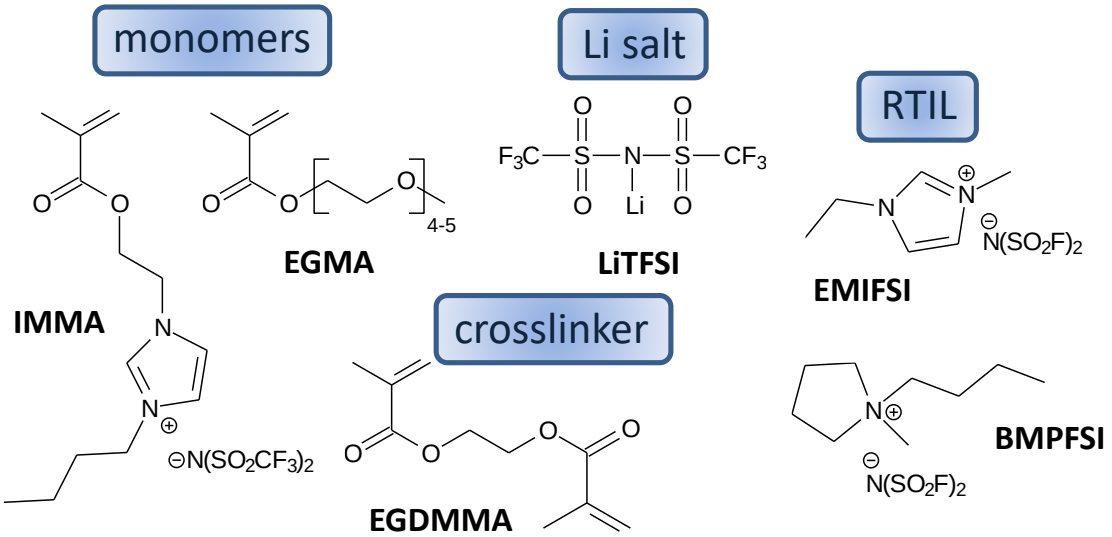

Scheme I: Chemical structures of the electrolytes' components

Table 1. Gel electrolyte composition (wt.%), thermal stability (T_5) in air, elastic shear modulus (G´), 0.1 Hz and 0.1% strain, and strain (%) at which G'=G" at 1 Hz and 25 ºC.

Electrolyte	monomers		LiTFSI wt. %	RTIL wt.%	TGA T_5 (ºC)	G´ (Pa)	G'=G" 1 Hz Strain %
	IMMA wt. %	EGMA wt.%					
PEGMA	-	30.8	0	69.2	238	2411	>100
PEGMA/Li	-	24.5	20.2	55.3	228	3382	56
PIMMA	30.8	-	0	69.2	296	1704	21
PIMMA/Li	24.5	-	20.2	55.3	235	1290	24
PIMMA/MIX*	30.8	-	0	69.2	296	-	-
PIMMA/MIX/Li*	24.5	-	20.2	55.3	247	-	-
COPO	23.1	7.7	0	69.2	272	1655	70
COPO/Li	18.4	6.1	20.2	55.3	227	1897	27

*electrolytes PIMMA/MIX and PIMMAMIX/Li contain a 1:1 wt. mixture of EMIFSI and BMPFSI. In the rest the RTIL is EMIFSI

2.2 Characterization

2.2.1 ATR-FTIR. IR spectra were recorded on the surface of the electrolytes using a PerkinElmer BX-FTIR spectrometer coupled with a MIRacle™ ATR accessory from PIKE Technologies, with 10 scans and resolution 2 cm^{-1}.

2.2.2 Thermogravimetric analysis (TGA) measurements were carried out in a TA Q-500 under air atmosphere, from 25 to 800 ºC at a heating rate of 10 ºC min^{-1}. The samples for TGA were small films of about 30 mg. The decomposition temperatures that resulted in 5% weight loss (T_5) appear listed in Table 1.

2.2.3 NMR

2.2.3.1.^{1}H-NMR and ^{13}C-NMR in solution. Intermediates and monomers were characterized by ^{1}H-NMR and ^{13}C-NMR spectra recorded on a *Varian-Mercury* 400 MHz using DMSO-d_6 as the solvent. The chemical shifts (δ) are given in section 2.1.2.

2.2.3.2. PFG-NMR. ^{13}C, ^{7}Li and ^{19}F PFG NMR measurements. The C-13 labeled carbon dioxide and ion diffusion NMR measurements were performed in a Bruker Avance™ 400 spectrometer equipped with a 89 mm wide bore, 9.4 T superconducting magnet (Larmor frequencies of ^{13}C, ^{7}Li and ^{19}F at 110.61, 155.51 and 376.51MHz, respectively). The diffusion reported data were acquired at 25 ± 0.1 ºC with a Bruker diffusion probe head, Diff60, using 90º radiofrequency (rf) pulse lengths of 10-12 µs. Several replicas of each sample were measured and the average value is reported.

To perform the NMR measurements of carbon dioxide diffusion coefficient, gel strips less than 2 mm wide and approximately 15 mm long were placed inside a 10 mm o.d. NMR tube designed for NMR studies of moderately pressurized gases. Prior to fill the tube at a given pressure with [^{13}C]O_2, the air was removed by vacuum. The gas pressure used in these experiments was 0.29 MPa to facilitate the measurements with adequate signal-to-noise ratio in a reasonable amount of time. The gas pressure was monitored with a transducer working in the range 0 - 1 MPa.

In the case of ^{7}Li and ^{19}F PFG NMR measurements, gel strips with the dimensions specified above were placed in a 5 mm o.d. NMR tube.

To determine the diffusion coefficients of interest, a pulsed field gradient stimulated spin echo pulse sequence was used.[21] The time between the first two 90º rf pulses (the echo time), τ_1, was 39 ms and the self-diffusion coefficients of $[^{13}C]O_2$, Li, TFSI and FSI were measured varying the amplitude of the gradient pulse between 0 and up to a maximum of 1,800 G cm^{-1}, when needed. The diffusion time and length of the gradient pulses were 80 and 2 ms, respectively. The repetition rate was always five times the spin-lattice relaxation time, T_1, of the nuclei being observed. The total acquisition time for these experiments varied from 10 min to 20 h. The decay of the echo amplitude was monitored typically to, at least 50% of its initial value and the apparent diffusion coefficient was calculated by fitting a mono-exponential function to the decay curve. Previously, the magnetic field gradient was calibrated as described elsewhere.[22]

2.2.4. Rheological measurements.

Rheology was performed at 25 ºC using an Advance rheometer AR2000 with a 20 mm steel crosshatched plate under nitrogen flow to avoid oxidative degradation. Oscillatory frequency sweeps were performed in the frequency range of 10^{-2}–10^2 Hz at 0.1% strain and in the % strain range of 10^{-2}–10^2 at 1 Hz. The % strain at which G'=G" in 1 Hz experiments and the value of G' in 0.1% strain experiments appears in Table 1.

2.2.5. Electric Measurements.

The conductivity of the electrolytes was determined by dielectric thermal analysis (DETA) with a NOVOCONTROL GmbH Concept 40 broadband dielectric spectrometer in the temperature range −50 °C to 90 °C and in the frequency range 1 to 10^7 Hz. The membranes were inserted between two gold-plated flat electrodes and the samples are cooled to −50 °C. Then, a frequency sweep was done every 10 °C heating from −50 to 90 °C, thereafter the same measurements are done but cooling from 90 to 25 °C. Ionic conductivity (σ) of the samples was calculated by using the conventional methods based on the Nyquist diagram and the phase angle as a function of the frequency plot. In a.c. measurements, the Nyquist diagram is obtained by representing the imaginary

part of the impedance (–Z”) versus the real part (Z’). This should give a semicircle of diameter R (being R the resistance of the sample) and center (R/2, 0). Then, the conductivity is given by σ= (l/R)·(l/S), being l the thickness of the sample and S the area of the section. Moreover, the same value of σ is obtained by plotting the real part of the conductivity (σ’) versus the frequency, being σ=σ’ when σ’ becomes practically constant with frequency, or more exactly at the frequency where tan δ is maximum or -Z” is minimum, being tan δ= Z´/-Z”. A selection of Nyquist plots and of σ’ versus the frequency at different temperatures is shown in Figure S1 in the Supplementary Information. The values of σ which appear in this work correspond to the second on cooling σ measurement.

3. Results.

Three pairs of electrolytes with and without LiTFSI were prepared using EMIFSI as liquid phase: the homopolymer with imidazolium pendant groups (named hereafter PIMMA and PIMMA/Li), the homopolymer with ethylene glycol pendant groups (PEGMA and PEGMA/Li) and a copolymer of both (COPO and COPO/Li). Ethylene glycol side groups as in PEGMA were chosen to ensure high dissolution of the LiTFSI. Another pair of electrolytes was prepared with PIMMA, but introducing a fraction of BMPFSI in the liquid phase (PIMMA/MIX and PIMMA/MIX/Li), to study the effect of increasing the liquid phase viscosity (η) on ion diffusivity and ionic conductivity (σ).

The electrolytes´ composition, thermal stability (as T_5) and rheological behaviour appears in Table 1. The membranes in this work are remarkably stable when heated in air, their thermal stability is similar, being T_5 lower in the electrolytes with LiTFSI, but always over 230 ºC. The TGA curves of the electrolytes appear in Figure S2 in the Supplementary Information. All the gel electrolytes in Table 1 are free-standing solids at 25 ºC, as evidenced by the pictures and the rheological curves in Figure 1. The softest materials are the pure polycationic membranes, PIMMA, PIMMA/Li, PIMMA/MIX

and PIMMA/MIX/Li, with G'≈1400 Pa, while the polymethacrylates PEGMA and PEGMA/Li are more rigid, with G'>2400 Pa, being the copolymers COPO and COPO/Li intermediate between both, with 1500<G'<2000 (see Figure 1a and G´ in Table 1). Figure 1b shows the self-standing character of the membranes, which can be manipulated without special precautions. Figure 1c represents the oscillatory stress as a function of the strain for the ion gels, at 25 ºC and 1 Hz. Under these conditions, the electrolytes display linear viscoelasticity up to strain values over 15%. Table 1 collects the values of strain for the G'-G" crossover at 1 Hz and 25 ºC.

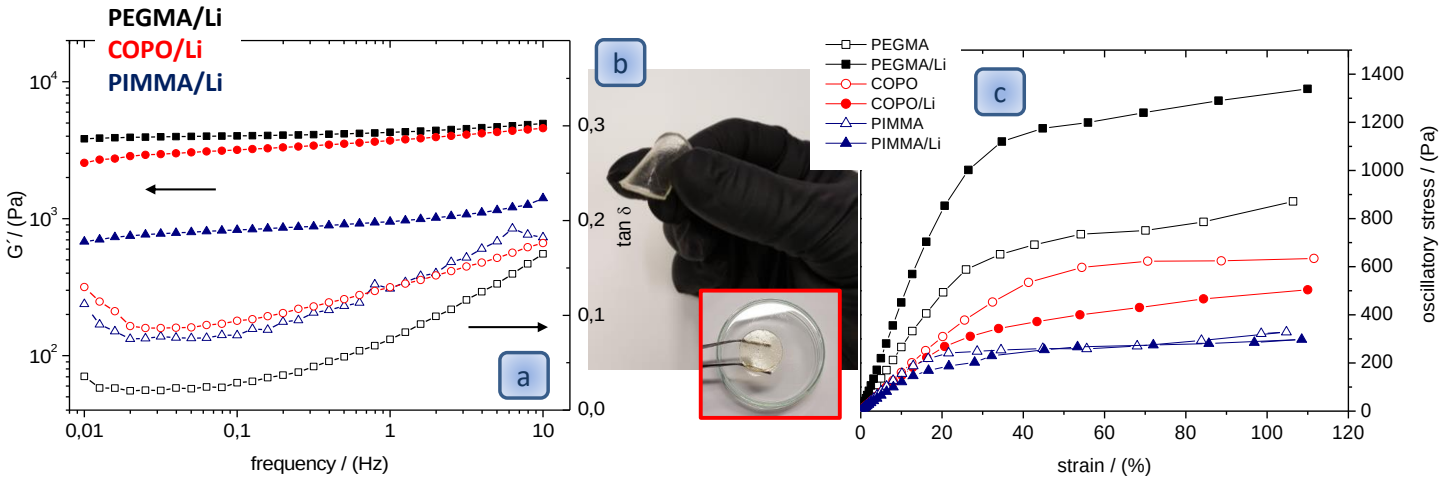

Figure 1. Rheology characterization and mechanical behavior of the gel electrolytes at 25 ºC: (a) elastic shear modulus (G´) (left) and tan δ (right) as a function of frequency, (b) pictures showing the self-standing ion gels and (c) oscillatory stress at 1 Hz as a function of strain.

All gels are soft but can be handled, and it has been possible to measure their σ in the temperature range –50 to 90 ºC. Figure 2 represents σ as a function of temperature on heating from –50 to 90 ºC for some of the ion gels. The data are well fitted to a Vogel-Fulcher-Tammann equation as can be expected in this type of electrolytes. The fitting parameters can be found in Table S1 of the Supplementary Information. No phase transitions are detected, indicating that the crystallization of the liquid phase is

hindered, what is confirmed by the absence of melting or crystallization processes in the membranes DSC (shown in Figure S3 in the supplementary information) in the temperature range under study.

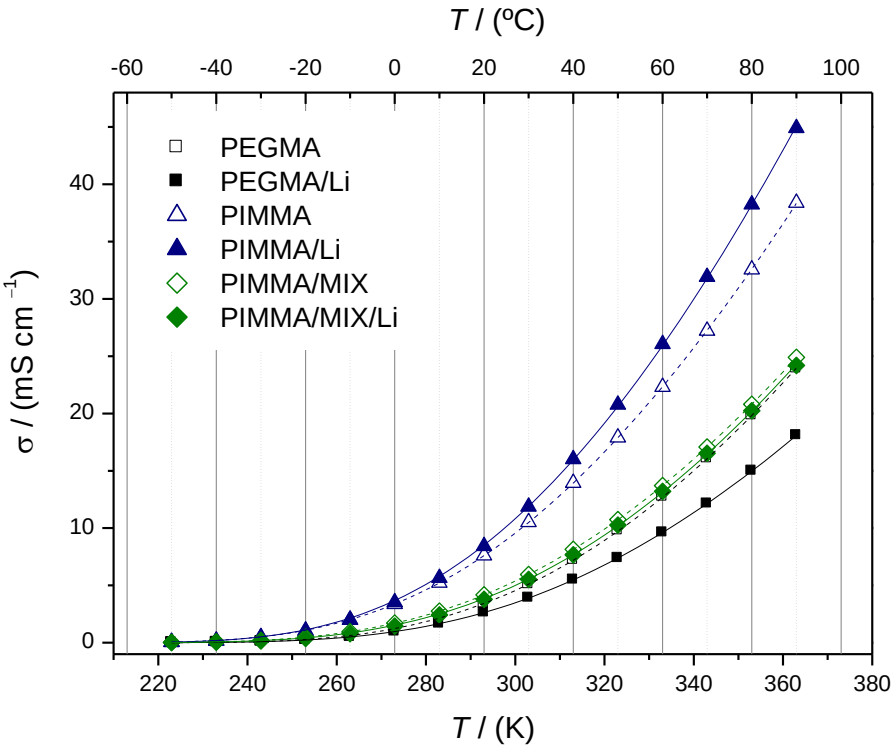

Figure 2. Conductivity (σ) as a function of temperature for some of the electrolytes and its fitting to Vogel-Fulcher-Tamman equation

The values of σ at 25 ºC are listed in Table 2. See how σ values are in the range of those characteristic of liquid electrolytes, as expected in this type of gel membranes. Compare, for example, the conductivity at 25ºC of liquids like EMIFSI (15.4 mS cm^{-1}, obtained in this work), or the 0.9 mol kg^{-1} solution of LiFSI in 1-methyl-1-propylpyrrolidinium FSI (3 mS cm^{-1}),[23] with the conductivity of PEGMA/Li (σ≈3.2 mS cm^{-1}), PIMMA/MIX/Li (4.6 mS·cm^{-1}) or PIMMA/Li (10 mS cm^{-1}). In fact, the σ value of PIMMA/Li, σ ≈10 mS cm^{-1} at 25 ºC is to the best of our knowledge the highest reported to date in a solid electrolyte.[10, 14] The same goes for the σ_{Li}^{calc} reported in the Table

S2 of the Supplementary Information for this electrolyte, calculated using the D_{Li} values in Table 2 and the Nernst-Einstein equation, which is σ_{Li}^{calc}=1.4 mS cm^{-1} at 25 ºC.

Note that in PEGMA/Li σ is lower than in PEGMA, a well-known effect in Li^+ doped ionic liquids because of the electrolyte´s η increase caused by the addition of the Li salt even when FSI is the counteranion. [17]. On the contrary, in the rest of the membranes, PIMMA-PIMMA/Li, PIMMA/MIX-PIMMA/ MIX/Li and COPO-COPO/Li, σ stays roughly constant or it even increases when LiTFSI is added. However, the η of the liquid phases consisting of EMIFSI or BMPTFSI increases when adding LiTFSI, as shown in Table S2 of the Supplementary Information. To gain understanding on this peculiar behavior, the diffusion coefficients (D) of TFSI, FSI and Li^+ were determined at 25 ºC by PFG-NMR and they appear in Table 2. In agreement with σ, the ions' D is maximum in PIMMA/Li, very especially in the case of Li^+, D_{Li}=37×10^{-11} m^2 s^{-1}, the highest reported to date in self-standing polymer-based electrolytes, to the best of our knowledge. In fact, in PIMMA/Li D_{Li} is even higher than D_{FSI} (×1.4) and D_{TFSI} (×1.8), again a very rare behavior in viscosity-governed Li electrolytes. As mentioned in the introduction, Li^+ has a characteristic large solvation shell [11] and consequently D_{Li} is smaller than its counteranions.[12, 13]

Table 2: Conductivity (σ) and diffusivity (D) of the electrolytes at 25 ºC.

Sample	σ (mS cm^{-1})	10^{12} D (m^2 s^{-1})		
		TFSI	FSI	Li^+
PEGMA	4.2	-	16.7	-
PEGMA/Li	3.2	9.7	12.0	1.5
PIMMA	8.9	20.5	24.4	-
PIMMA/Li	10.0	20.5	25.9	37.0
COPO	3.6	16.8	20.2	-
COPO/Li	3.5	16.8	21.0	20.9

PIMMA/MIX	5.0	14.3	16.6	-
PIMMA/MIX/Li	4.6	14.4	17.8	24.9

The closest results in the literature,[16] report $D_{Li}>D_{FSI}$ when [LiFSI]>1.6 mol kg^{-1} at T=60 ºC in high Li^+ content PMPFSI liquid electrolytes. Even in this case, D_{Li} is only slightly higher than D_{FSI}, with ratios $D_{Li}/D_{FSI}\approx1.1$ for values of $D_{Li}\approx20\times10^{-12}$ m^2 s^{-1}. Note that here we report $D_{Li}/D_{FSI}\approx1.4$ for $D_{Li}\approx37\times10^{-12}$ m^2 s^{-1}, at 25 ºC, at a lower [Li^+] of 0.8 mol kg^{-1} and in a solid electrolyte. The fact that D_{Li} in COPO/Li is intermediate between PIMMA/Li and PEGMA/Li, points to a connection between the molar fraction of IMMA in the ion gel polymer scaffold (χ_{IMMA}), and the strong increase of D_{Li}. Figure 3 shows that D_{Li}, D_{FSI} or D_{TFSI} increase linearly with χ_{IMMA}. As the slope of the dependence is much higher for Li^+ than for the anions FSI and TFSI, D_{Li} becomes higher than D_{TFSI} and D_{FSI} for χ_{IMMA}>60%. Figure 3 also illustrates the other peculiar feature of the electrolytes containing IMMA, which was mentioned before: the diffusion coefficients of the anions do not decrease on adding LiTFSI. See how D_{FSI} in PIMMA/Li or COPO/Li is higher than in PIMMA or COPO respectively (and D_{TFSI} the same), while both are lower in Li doped PEGMA gels in Table 2, which behave as conventional organic Li^+ electrolytes.

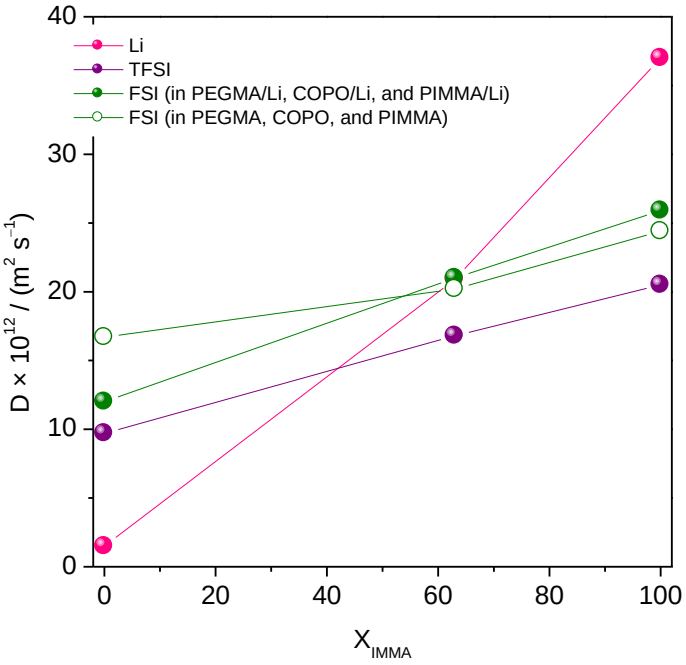

Figure 3. Diffusion coefficients (D) as a function of the molar fraction of IMMA (X_{IMMA}) in the gels. Lines are guides for the eyes.

Several experiments were carried out to understand better the behavior depicted in Figure 3. On the first place a new pair of electrolytes was prepared using the same polycationic scaffold as in PIMMA-PIMMA/Li, but employing a higher η liquid phase, the pair PIMMA/MIX-PIMMA/MIX/Li in Table 1. Though all D are lower than in the PIMMA-PIMMA/Li pair (as corresponds to a η-controlled diffusion), again D_{Li} is higher than D_{FSI} and D_{TFSI}, in particular 1.4 times over the former and 1.7 times over the latter, the same ratio as in the PIMMA-PIMMA/Li pair. This new experiment proves first, that the diffusivity in the electrolytes containing IMMA is to a certain extent ruled by the η of the liquid phase, and second, that the presence of IMMA is responsible for the peculiar high D_{Li} values.

To understand the effect of IMMA on the diffusivity of a neutral species, a second experiment was done consisting on measuring the diffusivity of CO_2 in PIMMA/Li and PEGMA/Li gels by PFG-NMR at 25 ºC and 3 bar. Contrary to what happens with D_{Li},

$D(CO_2)$ is very similar in PIMMA/Li, 14.5×10^{-11} m^2 s^{-1} and in PEGMA/Li, 15.4×10^{-11} m^2 s^{-1}, and in the range of what can be expected according to the literature.[24] This indicates that PEGMA/Li and PIMMA/Li, with the same liquid phase consisting on LiTFSI doped EMIFSI, are similar in the regard of molecular diffusivity, what points to some specific difference between both electrolytes affecting ionic (in particular Li^+) but not molecular transport.

Other authors[15, 16] have suggested the contribution of an anion exchange mechanism to the Li^+ transport in specific electrolytes containing FSI. Similitudes are seen between the FSI and TFSI FTIR spectra in those electrolytes,[9, 16] and the spectra of the electrolytes described in this work, which appear in Figure 4. In Figure 4a the FTIR spectra of the υ(S-N) region of FSI and TFSI in PEGMA-PEGMA/Li, COPO-COPO/Li and PIMMA-PIMMA/Li appear. This vibration is related to the aggregation state of the anions.[25] On Figure 4b, the same region is shown for the pure compounds EMIFSI, LiTFSI, EMITFSI and LiFSI. The spectral region of FSI in the PEGMA electrolyte (green) is composed of a broad band at 726 cm^{-1} due to FSI (as in EMIFSI, see Figure 4b); the addition of LiTFSI in PEGMA/Li makes the FSI component at 726 cm^{-1} to decrease, and a component close to 758 cm^{-1} to appear, this component being due to FSI as in LiFSI (see Figure 4b). The FTIR spectrum of TFSI in LiTFSI shows a component at 747 cm^{-1} (see Figure 4b) which is small but visible in the spectrum of PEGMA/Li. This spectrum contains also a band at 740 cm^{-1} and a component at 762 cm^{-1}, both related to TFSI as in EMITFSI (see Figure 4b).

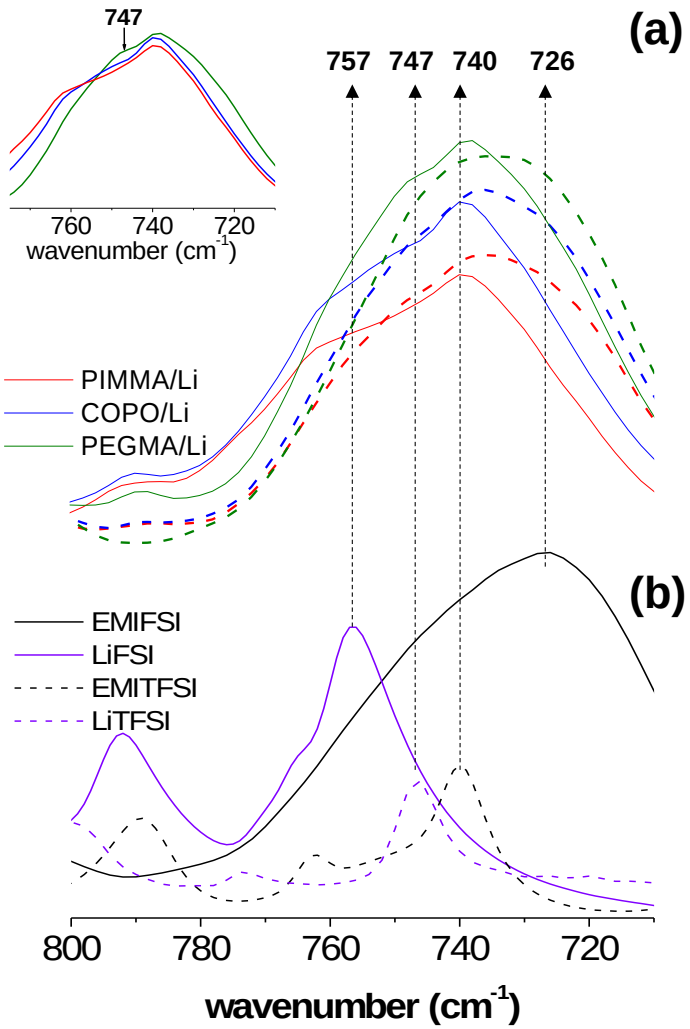

Figure 4: (a) FTIR spectra of the electrolytes with (solid lines) and without (dotted lines) LiTFSI in the region 800 to 710 cm^{-1} and (b) of EMIFSI, EMITFSI, LiTFSI and LiFSI in the same region

These results reveal that the mobile phase in PEGMA/Li gels is constituted by $Li(FSI)_x$ dispersed in a mixture of EMIFSI and EMITFSI, and some remaining LiTFSI clusters. On their turn, COPO/Li (blue) and PIMMA/Li (red) FTIR spectra indicate that as χ_{IMMA} increases (from PEGMA/Li to COPO/Li and finally to PIMMA/Li) the component at 747 cm^{-1} (TFSI as in LiTFSI) disappears almost completely (see inset in Figure 4b) and instead the component at 758 cm^{-1} (FSI as in LiFSI) becomes progressively stronger. So as χ_{IMMA} increases (PIMMA/Li>COPO/Li>PEGMA/Li) on one hand LiTFSI is better

dissociated and on the other a greater fraction of $Li(FSI)_x$ is formed. It has been reported before that polycationic chains promote the LiTFSI dissolution.[13]

4 Discussion

According to other authors,[15] Li^+ coordination to FSI propitiates that over a given (high) concentration of Li salt, Li^+ transport may occur via an anion-exchange activated mechanism, what brings about D_{Li} values over those obtained when only η controlled diffusion occurs, to the point of surpassing those of the anions in the electrolyte. In the electrolytes described in this work the remarkable predominance of D_{Li} over D_{FSI} seems to depend, not on surpassing a given threshold of $[Li^+]$ as described in [15], but on increasing the χ_{IMMA} in the polymer scaffold. It has to be borne in mind that in the IMMA containing electrolytes the local $[Li^+]$ can be substantially higher than the nominal one, because of i) the repulsion of Li^+ away from the polycationic chains, what will depend on χ_{IMMA} and ii) because of the high dissociation of the LiTFSI salt, which also depends on χ_{IMMA} as shown in the inset of Figure 4b and reported previously by other authors.[13] Scheme II illustrates the proposed organization of the liquid phases in PEGMA/Li and in PIMMA/Li.

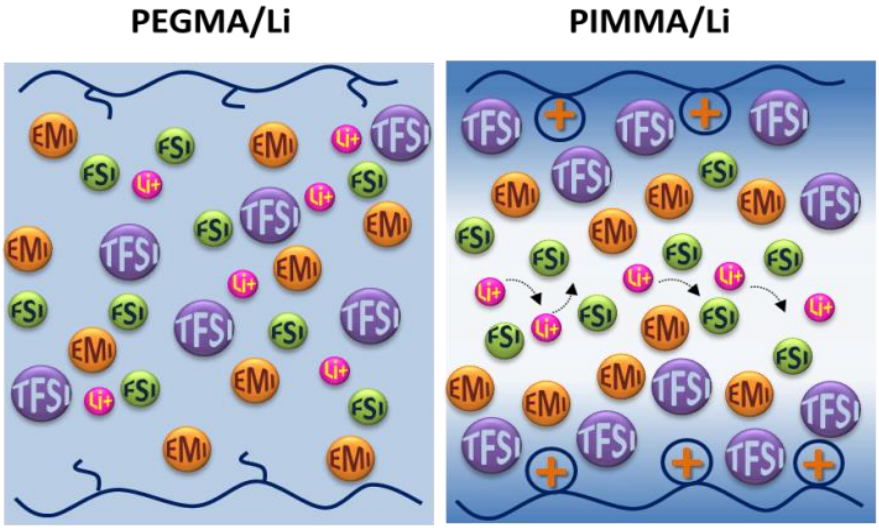

Scheme II: Proposed organization of the liquid phase in PEGMA/Li and PIMMA/Li.

The liquid phase in PIMMA/Li can be thought of as an organised liquid where Li^+ is localised away from the PIMMA scaffold, and coordinated to FSI, as suggested by the FTIR and the literature, while TFSI rather neutralises the cationic PIMMA chain and EMI cations (which is also coordinated to FSI). This organization favours a high local $Li(FSI)_x$ concentration. Then, the dependence of the D_{Li} on χ_{IMMA} may actually be a dependence on the local $[Li^+]$, and the high D_{Li} values may arise from the contribution of the anion exchange transport mechanism for Li^+. This is the first evidence of an anion exchange mechanism contributing to Li^+ diffusion and resulting in high conductivity in a solid electrolyte.

Certainly, a mixed transport mechanism, partly η controlled, partly anion-exchange could be taking place in the electrolytes containing IMMA and would explain liquid-like D_{Li} values of about 4×10^{-11} m^2 s^{-1} at 25 ºC, significantly higher than those of FSI or TFSI in the same electrolyte, $\approx2\times10^{-10}$ m^2 s^{-1}, and the subsequently high σ≈10 mS cm^{-1} at 25 ºC, unreported to date in similar electrolytes. Self-standing ion gel polymer electrolytes with such Li^+ mobilities deserve close attention as future electrolytes in Li batteries.

Conclusions

Polymer ion gel electrolytes constituted by a liquid phase comprising EMIFSI/LiTFSI ionic liquid and a scaffold made of PIMMA have been prepared. The electrolytes are self-standing gels, thermally stable, and show a very remarkable ionic conductivity of up to 10 mS cm^{-1} at 25 ºC, i.e. really like a chemically analogous liquid electrolyte. Such high conductivities, unreported to date in solid electrolytes, are related to the high diffusivity of the ions in the electrolyte. In particular, at low Li salt concentration and 25 ºC, D_{Li} which are significantly higher than D_{FSI} and D_{TFSI} have been measured, a result unreported so far. It is proposed that in these polycationic electrolytes Li^+ transport involves, together with conventional viscosity governed-diffusion, a net contribution of

an anion exchange mechanism, promoted by the high local concentration of $Li(FSI)_x$ species. The high local $Li(FSI)_x$ is caused by the repulsion of Li^+ away from the polycationic chain and by the high dissociation of the LiTFSI salt. This is the first evidence of an anion exchange mechanism contributing to Li^+ diffusion and conductivity in a solid electrolyte. This combined transport mechanisms increases D_{Li} up to liquid-like values and over D_{anions}, and makes these polycationic solid electrolytes a very attractive choice for their study in actual Li^+ batteries.

Acknowledgements This study was supported by Comunidad de Madrid (Project Ref. LIQUORGAS-CM, S2013/MAE-2800). Authors are grateful to Francisco González González for the determination of the liquid electrolytes' viscosity.

References

[1] R.C. Agrawal, G.P. Pandey, Solid polymer electrolytes: materials designing and all-solid-state battery applications: an overview, Journal of Physics D: Applied Physics, 41 (2008) 223001.
[2] M. Marcinek, J. Syzdek, M. Marczewski, M. Piszcz, L. Niedzicki, M. Kalita, A. Plewa-Marczewska, A. Bitner, P. Wieczorek, T. Trzeciak, M. Kasprzyk, P.Łężak, Z. Zukowska, A. Zalewska, W. Wieczorek, Electrolytes for Li-ion transport – Review, Solid State Ionics, 276 (2015) 107-126.
[3] R. He, T. Kyu, Effect of Plasticization on Ionic Conductivity Enhancement in Relation to Glass Transition Temperature of Crosslinked Polymer Electrolyte Membranes, Macromolecules, 49 (2016) 5637-5648.
[4] A. Mejía, N. García, J. Guzmán, P. Tiemblo, Thermoplastic and solid-like electrolytes with liquid-like ionic conductivity based on poly(ethylene oxide) nanocomposites, Solid State Ionics, 261 (2014) 74-80.
[5] A. Mejía, N. García, J. Guzmán, P. Tiemblo, Extrusion processed polymer electrolytes based on poly(ethylene oxide) and modified sepiolite nanofibers: Effect of composition and filler nature on rheology and conductivity, Electrochim. Acta, 137 (2014) 526-534.
[6] A. Mejía, S. Devaraj, J. Guzmán, J.M. Lopez Del Amo, N. García, T. Rojo, M. Armand, P. Tiemblo, Scalable plasticized polymer electrolytes reinforced with surface-modified sepiolite fillers - A feasibility study in lithium metal polymer batteries, J. Power Sources, 306 (2016) 772-778.
[7] E.H. Cha, S.A. Lim, J.H. Park, D.W. Kim, D.R. Macfarlane, Ionic conductivity studies of gel polyelectrolyte based on ionic liquid, J. Power Sources, 178 (2008) 779-782.
[8] A. Mejía, E. Benito, J. Guzmán, L. Garrido, N. García, M. Hoyos, P. Tiemblo, Polymer/Ionic Liquid Thermoplastic Electrolytes for Energy Storage Processed by Solvent Free Procedures, ACS Sustainable Chem. Eng., 4 (2016) 2114-2121.

[9] K. Fujii, S. Seki, H. Doi, Y. Umebayashi, Structural Aspect on Li Ion Solvation in Room-Temperature Ionic Liquids, in: A.A.J. Torriero (Ed.) Electrochemistry in Ionic Liquids: Volume 1: Fundamentals, Springer International Publishing, Cham, 2015, pp. 317-332.
[10] E. Simonetti, M. Carewska, G. Maresca, M. De Francesco, G.B. Appetecchi, Highly conductive, ionic liquid-based polymer electrolytes, J Electrochem Soc, 164 (2017) A6213-A6219.
[11] J. Pitawala, A. Martinelli, P. Johansson, P. Jacobsson, A. Matic, Coordination and interactions in a Li-salt doped ionic liquid, J. Non-Cryst. Solids, 407 (2015) 318-323.
[12] M. Brinkkötter, E.I. Lozinskaya, D.O. Ponkratov, P.S. Vlasov, M.P. Rosenwinkel, I.A. Malyshkina, Y. Vygodskii, A.S. Shaplov, M. Schönhoff, Influence of anion structure on ion dynamics in polymer gel electrolytes composed of poly(ionic liquid), ionic liquid and Li salt, Electrochim. Acta, 237 (2017) 237-247.
[13] R. Bhandary, M. Schönhoff, Polymer effect on lithium ion dynamics in gel polymer electrolytes: Cationic versus acrylate polymer, Electrochim. Acta, 174 (2015) 753-761.
[14] A.S. Shaplov, R. Marcilla, D. Mecerreyes, Recent Advances in Innovative Polymer Electrolytes based on Poly(ionic liquid)s, Electrochim. Acta, 175 (2015) 18-34.
[15] J.B. Haskins, W.R. Bennett, J.J. Wu, D.M. Hernández, O. Borodin, J.D. Monk, C.W. Bauschlicher, J.W. Lawson, Computational and Experimental Investigation of Li-Doped Ionic Liquid Electrolytes: [pyr14][TFSI], [pyr13][FSI], and [EMIM][BF4], J. Phys. Chem. B, 118 (2014) 11295-11309.
[16] H. Yoon, A.S. Best, M. Forsyth, D.R. MacFarlane, P.C. Howlett, Physical properties of high Li-ion content N-propyl-N-methylpyrrolidinium bis(fluorosulfonyl)imide based ionic liquid electrolytes, Phys. Chem. Chem. Phys., 17 (2015) 4656-4663.
[17] S. Tsuzuki, K. Hayamizu, S. Seki, Origin of the Low-Viscosity of [emim][(FSO2)2N] Ionic Liquid and Its Lithium Salt Mixture: Experimental and Theoretical Study of Self-Diffusion Coefficients, Conductivities, and Intermolecular Interactions, J. Phys. Chem. B, 114 (2010) 16329-16336.
[18] M. Liras, O. Garcia, I. Quijada-Garrido, G. Ellis, H.J. Salavagione, Homogenous thin layer coated graphene via one pot reaction with multidentate thiolated PMMAs, J. Mater. Chem. C, 2 (2014) 1723-1729.
[19] H. Chen, J.-H. Choi, D. Salas-de la Cruz, K.I. Winey, Y.A. Elabd, Polymerized Ionic Liquids: The Effect of Random Copolymer Composition on Ion Conduction, Macromolecules, 42 (2009) 4809-4816.
[20] T. Ishikawa, M. Kobayashi, A. Takahara, Macroscopic Frictional Properties of Poly(1-(2-methacryloyloxy)ethyl-3-butyl Imidazolium Bis(trifluoromethanesulfonyl)-imide) Brush Surfaces in an Ionic Liquid, ACS Appl. Mater. Interfaces, 2 (2010) 1120-1128.
[21] E.O. Stejskal, J.E. Tanner, Spin diffusion measurements: Spin echoes in the presence of a time-dependent field gradient, J. Chem. Phys, 42 (1965) 288-292.
[22] L. Garrido, M. López-González, E. Saiz, E. Riande, Molecular basis of carbon dioxide transport in polycarbonate membranes, J. Phys. Chem. B, 112 (2008) 4253-4260.
[23] J. Vila, P. Ginés, J.M. Pico, C. Franjo, E. Jiménez, L.M. Varela, O. Cabeza, Temperature dependence of the electrical conductivity in EMIM-based ionic liquids, Fluid Phase Equilib., 242 (2006) 141-146.
[24] T.C. Lourenço, S. Aparicio, G.C. Costa, L.T. Costa, Local environment structure and dynamics of CO2 in the 1-ethyl-3-methylimidazolium bis(trifluoromethanesulfonyl)imide and related ionic liquids, J. Chem. Phys, 146 (2017) 104502.
[25] J.C. Lassegues, J. Grondin, D. Talaga, Lithium solvation in bis(trifluoromethanesulfonyl)imide-based ionic liquids, Phys. Chem. Chem. Phys., 8 (2006) 5629-5632.

Table of contents.

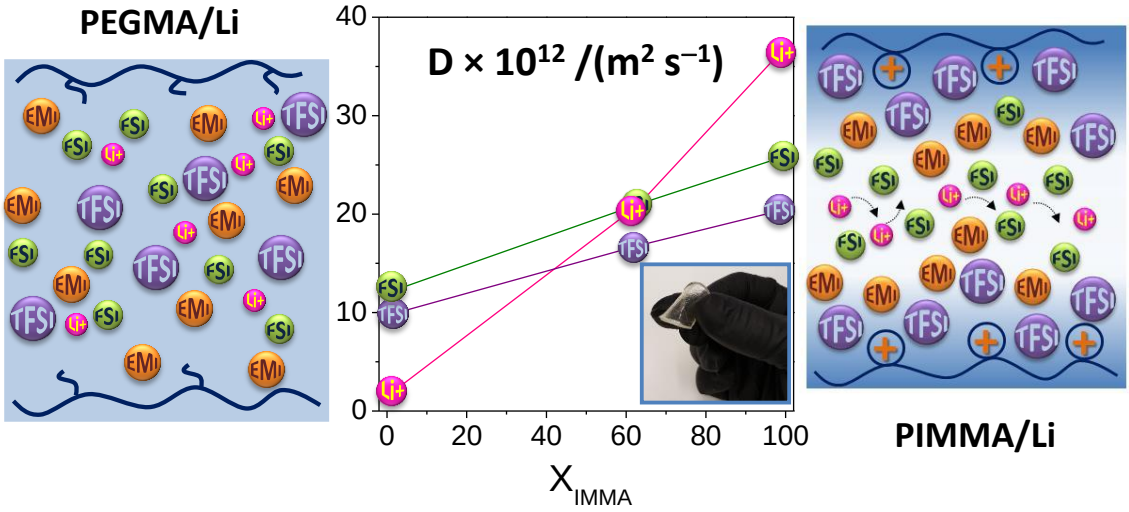

Supplementary Information of Highly efficient mixed Li^+ transport in ion gel polycationic electrolytes

Jesús L. Pablos, N. García, L. Garrido, J. Guzmán, F. Catalina, T. Corrales, P. Tiemblo

Instituto de Ciencia y Tecnología de Polímeros, Consejo Superior de Investigaciones Científicas, ICTP-CSIC, Juan de la Cierva 3, 28006 Madrid, Spain

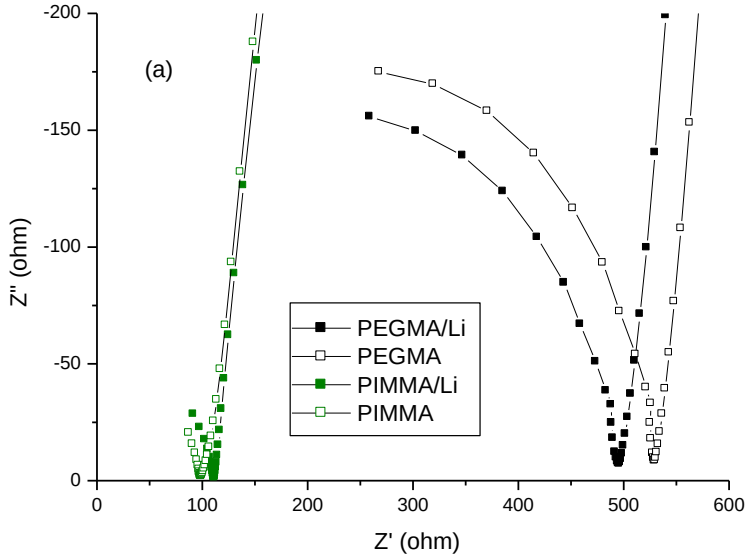

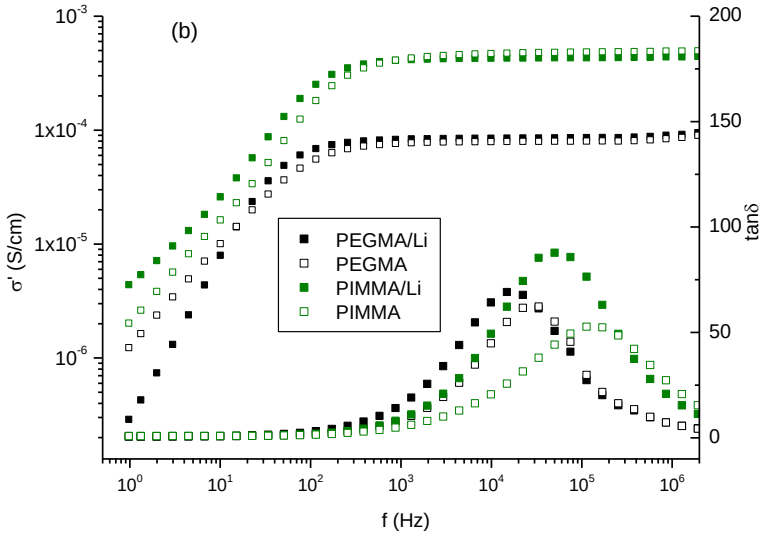

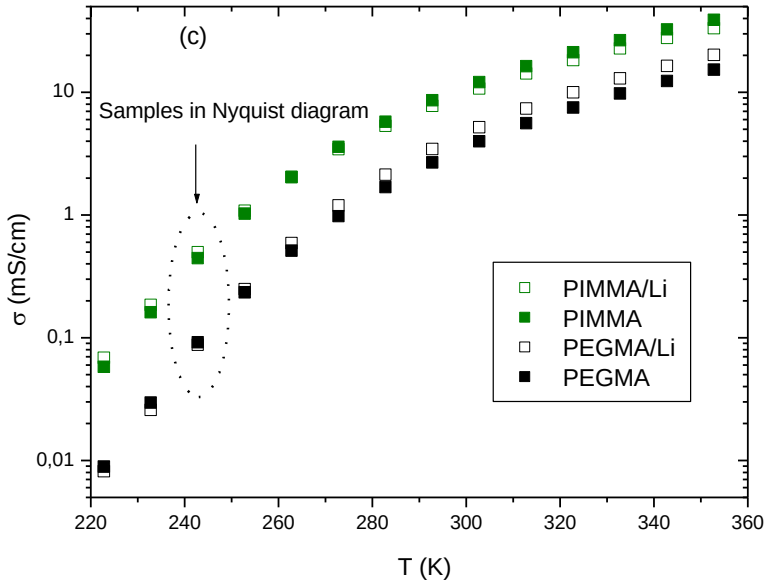

Figure S1: (a) Nyquist diagram of PIMMA/Li, PIMMA, PEGMA/Li and PEGMA at -30ºC. The temperature has been chosen so as to enable visualizing the four samples PIMMA/Li, PIMMA, PEGMA/Li and PEGMA in the same graph. (b) Real part of the conductivity (σ') and tan δ versus the frequency for PIMMA/Li, PIMMA, PEGMA/Li and PEGMA at -30ºC (c) conductivity as a function of temperature showing the samples in (a) and (b).

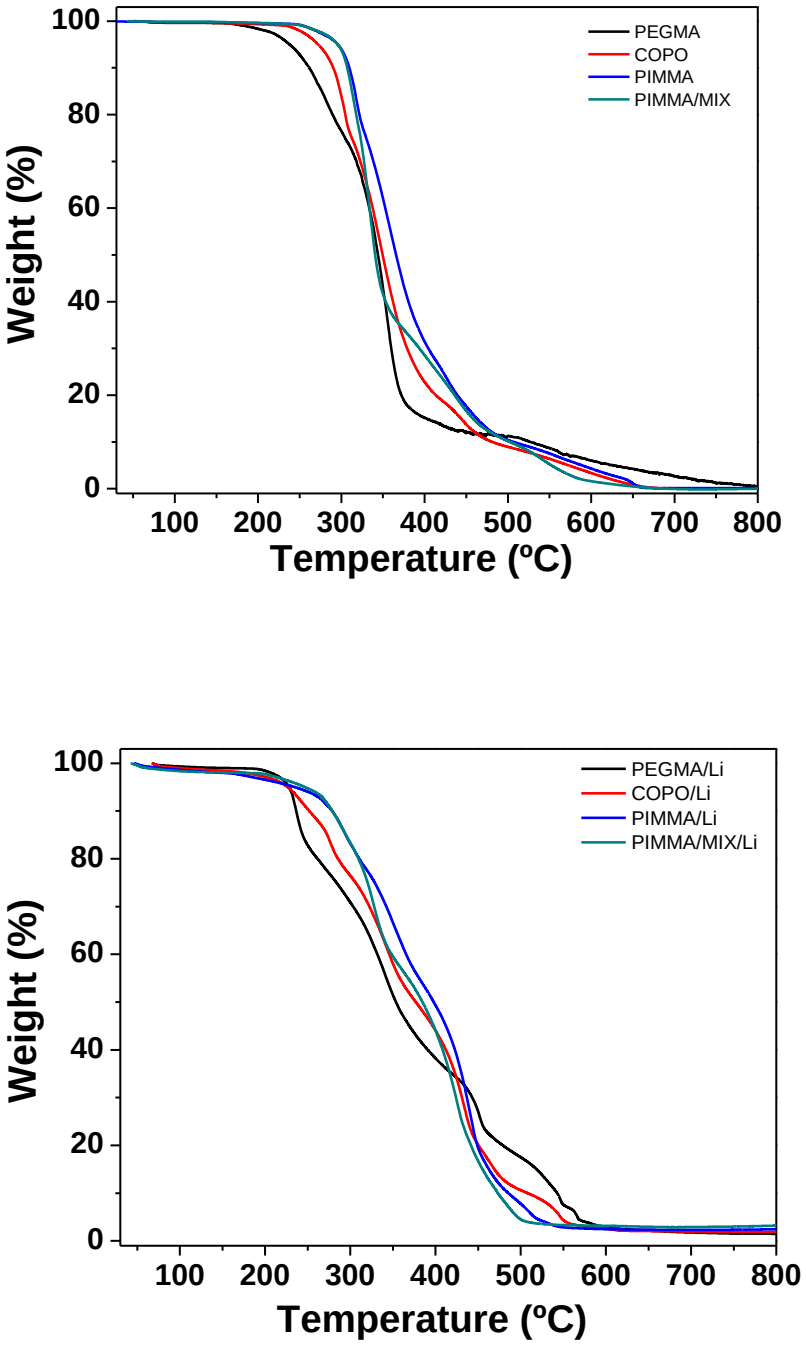

Figure S2: Thermogravimetric analysis of all the samples, without LiTFSI (up) and with LiTFSI (down). Experiments were done in air at a heating rate of 10 ºC min^{-1}.

TableS1. Vogel-Fulcher-Tammann parameters extracted from the fitting of the conductivity data as a function of temperature shown in figure 2.

sample	σ_∞ (mS cm^{-1})	B (K)	T_0 (K)
PEGMA	703	646	172
PEGMA/Li	660	721	162
PIMMA	977	680	153
PIMMA/Li	938	600	166
PIMMA/MIX	894	753	153
PIMMA/ MIX/Li	747	683	163

Differential Scanning Calorimetry (DSC) was performed on a METTLER DSC-823e instrument previously calibrated with an indium standard (T_m = 429 K, ΔH_m = 25.75 J g^{-1}). Film samples (10 mg) were measured under nitrogen atmosphere from –50ºC to 130 ºC at 10 ºC min^{-1}, the ionic liquids (EMIFSI and BMPFSI) were measured between –50ºC to 100 ºC. The third heating scan is represented in Figure S3.

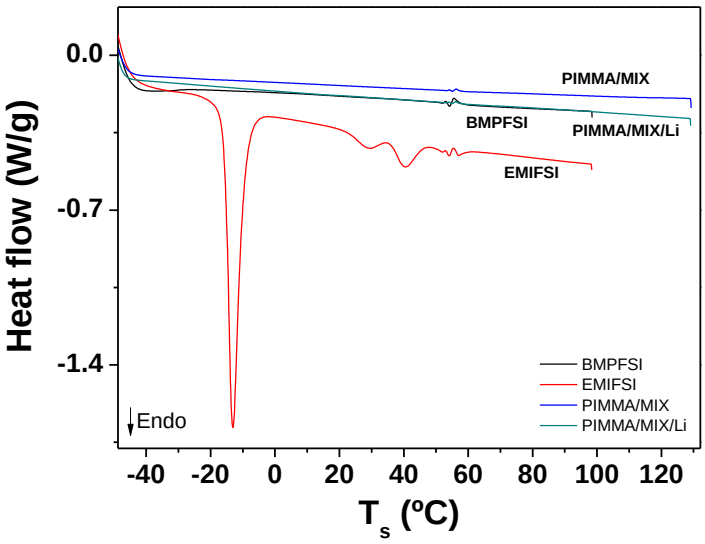

Figure S3: DSC heating scans of the ion gels PIMMA/MIX and PIMMA/MIX/Li and the ionic liquids EMIFSI and BMP FSI measured in nitrogen and at 10 ºC min^{-1}.

TableS2: Viscosity (η) of liquid electrolytes with analogous chemical composition to the different ion gels in this work (η_{liquid} see experimental details below), η_1 the mixtures without PEG chains and η_2 the mixtures with PEG chains. The $^*\sigma_{Li}^{calc}$ has been calculated with the Nernst-Einstein equation (Equation S1) and the hydrodynamic radius (r) with the Stokes-Einstein equation (EquationS2), as detailed below. All data are given at 25ºC.

Sample	$^*\sigma_{Li}^{calc}$ (mS cm^{-1})	η_1 (cP)	r_{Li_1} (nm)	r_{FSI_1} (nm)	r_{TFSI_1} (nm)	η_2 (cP)	r_{Li_2} (nm)	r_{FSI_2} (nm)	r_{TFSI_2} (nm)
PEGMA		19		0.68		74		0.18	
PEGMA/Li	0.06	44	3.32	0.42	0.51	104	1.40	0.18	0.22
PIMMA		19		0.46	0.55				
PIMMA/Li	1.37	44	0.13	0.19	0.24				
COPO		19		0.56	0.67	39		0.27	0.33
COPO/Li	0.84	44	0.24	0.24	0.30	66	0.16	0.16	0.20
PIMMA/MIX		28		0.47	0.54				
PIMMA/MIX/Li	0.90	86	0.10	0.14	0.18				

The viscosity (η) of the liquid phase (η_{liquid}) in each electrolyte has been determined at 25 ºC using an Anton Paar SVM 3000. These liquid phases have been prepared so as to mimic as far as possible the mobile phase in the gel electrolytes, and they have the same composition as their solid electrolyte analogue except for the polymer scaffold. For instance, in electrolytes PEGMA, COPO and PIMMA the liquid phase is simply EMIFSI, while in PIMMA/Li the liquid phase is a solution of EMIFSI:LiTFSI at the wt.% collected in Table 1 (η_1 in Table S2). For PEGMA, PEGMA/Li, COPO and COPO/Li, the liquid phase was also modeled adding methyl ether PEG chains of Mw=550 (η_2 in Table S2) at the following wt.% ratios: 50:50 EMIFSI:PEG for PEGMA, 50:17.5:32.5

EMIFSI:LiTFSI:PEG for PEGMA/Li, 68.5:31.5 EMIFSI:PEG for COPO and 62:17.5:20.5 EMIFSI:LiTFSI:PEG for COPO/Li emulating the electrolyte formulations.

With the D_{Li} obtained from NMR experiments and reported in Table S2, it is possible to estimate σ_{Li}^{calc} using the Nernst Einstein equation (Equation 2) for Li^+,

$$\sigma_{Li} = \frac{F^2}{RT} \cdot n_{LiTSFI} \alpha_{LiTFSI} \cdot D_{Li} \quad [S1]$$

where n_{LiTFSI} is the LiTFSI molar concentration and α_{LiTFSI} is its dissociation coefficient, which is assumed to be equal to one. The as obtained values are reported in the 2nd column in Table S2. Large differences are seen, with σ_{Li}^{calc} ranging from 0.06 mS cm^{-1} (PEGMA/Li) to 1.37 mS cm^{-1} (PIMMA/Li), which is really outstanding.

Using the D in Table 2 and the η_{liquid} data in TableS2, the hydrodynamic radius, r_i, were calculated for the available species making use of the Stokes-Einstein equation (Equation S2),

$$D_i = \frac{k_B T}{6\pi\eta r_i} \quad [S2]$$

where k_B is the Boltzmann constant and *T* the temperature. The results are reported in Table S2 (subindexes 1 and 2 stand for the use of η_1 or η_2, respectively). As reported before, because of its high charge density, Li^+ usually has a large solvation shell and large hydrodynamic radius. In conventional organic solvents, like EC or PC, the solvation shell of Li^+ comprises four carbonate molecules, in RTILs containing FSI or TFSI it has been published that the solvation shell consists of 4 to 2 TFSI or FSI (*J. Pitawala, A. Martinelli, P. Johansson, P. Jacobsson, A. Matic, Coordination and interactions in a Li-salt doped ionic liquid, J. Non-Cryst. Solids, 407 (2015) 318-323*). In any case, in solution, the Stokes radius of Li^+ is larger than that of FSI or TFSI, and D_{Li} is smaller than D_{FSI} or D_{TFSI}. However, for PIMMA/Li and PIMMA/MIX/Li, r_{Li} in Table S2 is smaller than that of the anions. On their turn, r_{FSI} or r_{TFSI} are very low but closer to the

range of values reported in the literature. The fact that the calculated r_{Li} in PIMMA/Li and PIMMA/MIX/Li are very similar suggests that, even if the η_{liquid} employed for the calculation are a mere approximation, they reproduce quite well the differences between both electrolytes.